

STOCHASTIC MODELLING AND ANALYSIS OF DYNAMIC PLASMA REFLECTION

Y. M. Zhang and Y. Ma

*Center for Robotics and Manufacturing Systems and
Department of Electrical and Computer Engineering
College of Engineering
University of Kentucky
Lexington, KY 40506, USA*

Abstract: Keyhole arc welding is a cost-effective process to weld thick materials. To successfully apply this process, the state of the keyhole must be accurately detected and used in feedback control. In this paper, the dynamic behavior of the plasma reflection is described using the reflection arc angle (RAA). It is found that the RAA series can be considered an autoregressive moving-average (ARMA) process. The parameters of the ARMA are recursively estimated using the extended least squares algorithm. It is found that the recursive estimates of the model parameters change as the state of the keyhole changes. A discriminator has been proposed to determine the state of the keyhole based on the recursive estimates of the model parameters. *Copyright © 2002 IFAC*

Keywords: Autoregressive moving average (ARMA), least squares algorithm, impulse transfer function.

1. INTRODUCTION

Fig. 1 demonstrates the behaviors of the plasma arc and its reflection during keyhole arc welding. When the keyhole is not fully penetrated, the plasma arc has to be reflected from the cavity which is referred to as non-penetrated keyhole. However, after the keyhole is fully established, the plasma jet will exit at the bottom of the penetrated keyhole. The amount of the reflected plasma, if any, will be significantly reduced. Hence, it is possible to reliably monitor the establishment of the penetrated keyhole based on the behavior of the reflected plasma.

As a preliminary verification, experiments have been done to monitor the establishment of the penetrated keyhole based on the reflection behavior of the plasma jet by attaching a detection metal cup (Fig. 2) (Zhang, et al.,2001). Experiments showed that the output of the sensor, which is proportional to the current of the detection loop, is large if the keyhole is not fully penetrated. However, after the keyhole is fully penetrated, the output of the sensor sharply drops (Fig.

2). This suggests that a simple but reliable sensor could be developed to monitor the establishment of the penetrated keyhole with no interference with the process.

Although the results in Fig. 2 experimentally verified the feasibility of monitoring the establishment of the penetrated keyhole based on the reflection behavior of the plasma arc, there is a lack of understanding of the plasma behavior. Without sufficient understanding of the dynamic behaviors of the plasma arc and its reflection, the accuracy and reliability of such a sensor would be difficult to assess.

To understand the dynamic behaviors of the plasma reflection, a high speed image system was used to observe the plasma arc and its reflection at a frame rate of 1,000 frames per second (Ma.,2001). The angle of the reflected plasma, referred to as reflection arc angle (RAA), was extracted. It was found that the development of the keyhole has three states or periods (Ma.,2001), the stable non-penetrated keyhole period, the instable transition period, and the stable penetrated keyhole period. During the stable non-penetrated

period, the RAA fluctuates around a small degree with small amplitudes. Once the development enters into the instable transition period, the RAA fluctuates around a larger degree with larger amplitudes. After the stable penetrated keyhole state is established, the RAA increases and is stabilized at an even larger degree.

Although the RAA exhibits a fundamental relationship with the state of the keyhole development, the determination of the state based on the RAA appears not straightforward because of the complexity of the dynamic behavior of the RAA. In this study, the RAA will be modeled as a stochastic process and the recursive estimate of the model parameters will be used to determine the state of the keyhole.

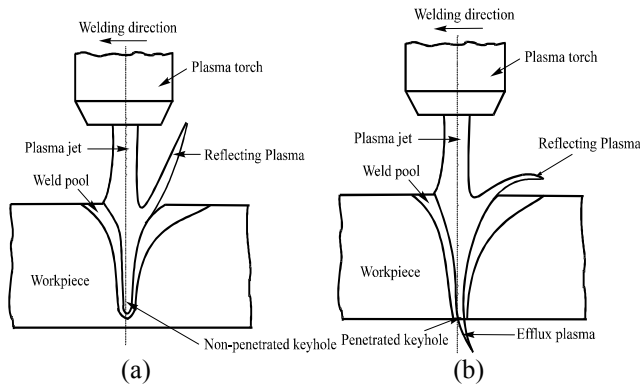


Fig. 1 Behaviors of plasma reflection. (a) Non-penetrated keyhole. (b) Penetrated keyhole.

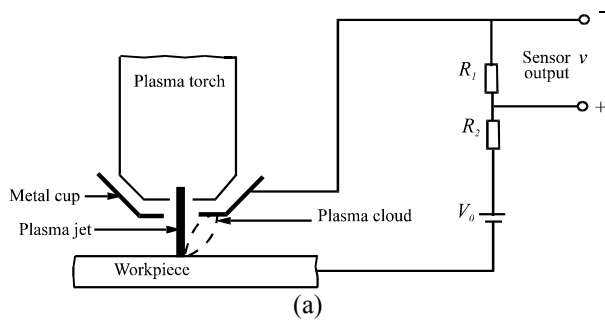


Fig. 2 A plasma reflection sensor. (a) Sensor schematic; (b) Sensor response in comparison with keyhole detection signal.

2. ARMA MODEL FOR RAA SERIES

Fig. 3 shows two types of the images. While the plasma arc and its reflection can be observed in both

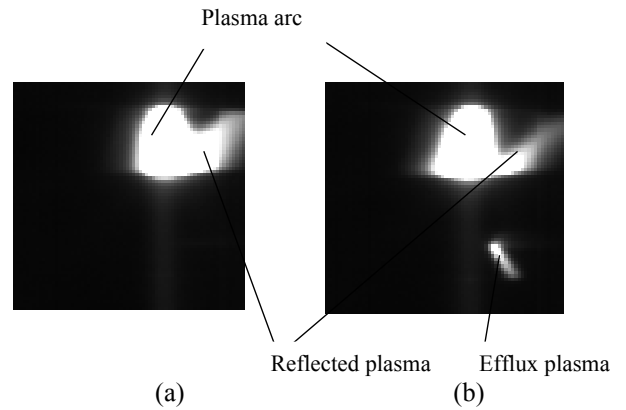


Fig. 3 Images of plasma arc and its reflection. (a) Non-penetrated keyhole; (b) Penetrated keyhole.

images, the efflux plasma can be observed only when the keyhole is fully penetrated.

Fig. 4 demonstrates the proposed method which is used to extract the RAA in this study. In the proposed method, the middle vertical axis of the main plasma arc, denoted as aa , is first identified by detecting the highest and lowest point in the image. Then the median points are referred to as effective points 1, 2, ..., 5 of the vertical lines $l_1 \dots l_5$. By utilizing the least square method and treating the effective points as the observation points (Ljung, 1997), the slope and intercept of the axis of the reflection arc can be obtained and used to generate the reflection arc angle \mathcal{G} . In particular, the regressive model for least square method is (Ljung, 1997):

$$\bar{Y} = \tilde{\Phi} \bar{\theta} \quad (1)$$

where $\bar{Y} = [y(1), \dots, y(5)]^T$, $\bar{\theta} = [b, k]^T$, $\tilde{\Phi} = \begin{bmatrix} 1, & \dots, & 1 \\ x(1), & \dots, & x(5) \end{bmatrix}^T$

and k and b are the slope and intercept respectively for the line equation of the axis of the reflected plasma. The least squares estimate of the parameter vector $\bar{\theta}$ is (Ljung, 1997):

$$\hat{\bar{\theta}} = (\tilde{\Phi}^T \tilde{\Phi})^{-1} (\tilde{\Phi}^T \bar{Y}) \quad (2)$$

Hence, the estimated RAA \mathcal{G} is:

$$\mathcal{G} = \tan^{-1}(k) \quad (3)$$

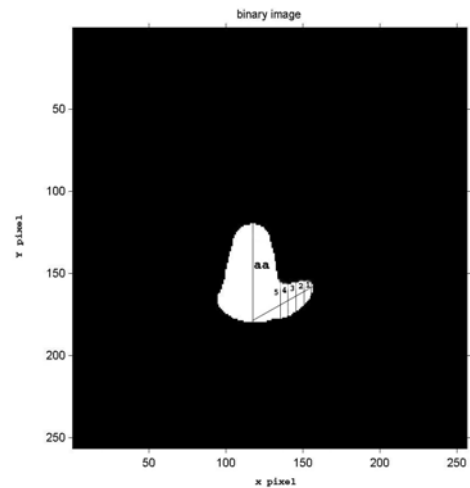
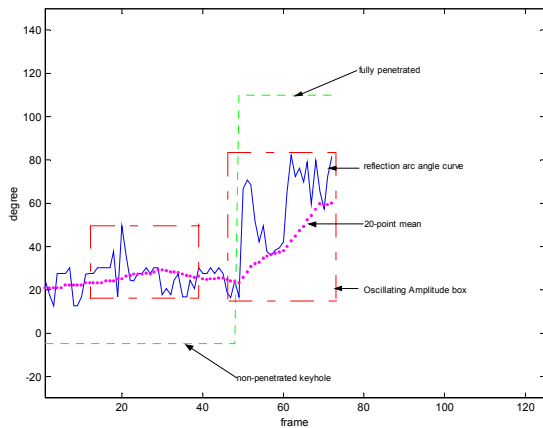


Fig. 4 Determination of reflection arc angle.

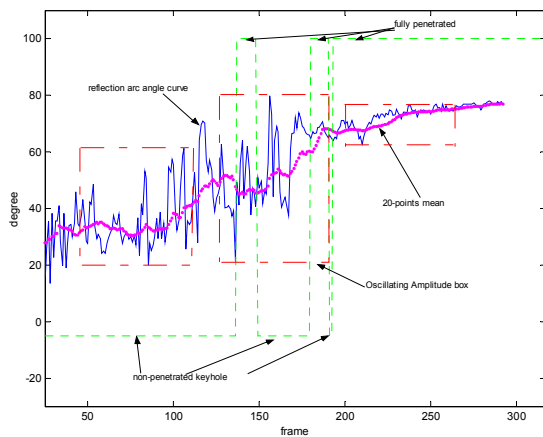
Consequently, a virtual reflection arc line can be drawn using the slope k and intercept b in the two-dimensional image as shown in Fig. 4.

Fig. 5 shows the RAA series obtained from two cases, one for welding 4.5 mm thick workpiece, and another for welding 6.5 mm thick workpiece. In both cases, the keyhole welding process changed from the initial non-penetrated keyhole mode to the penetrated keyhole mode. The algorithm described above used to obtain the RAA from the images.

Observation of the original images (Ma.,2001) shows that for the case of welding 4.5 mm thick workpiece, the first appearance of the efflux plasma, which indicates the penetrated keyhole, is at image frame 49. However, it appears that the reflected plasma only settles down after frame 62. In the case of 6.5 mm thick work-piece, the efflux plasma first occurs at the 113th frame. However, the efflux plasma remains always present only after the 169th frame. A previous analysis (Ma.,2001) showed that the development of the keyhole has three states or periods: the stable non-penetrated keyhole period during which the non-penetrated keyhole develops, the instable transition period during which the penetrated keyhole can be closed or a non-penetrated keyhole can become fully penetrated by slight disturbances, and the stable penetrated keyhole period in which the penetrated keyhole maintains. The



(a) 4.5 mm thickness



(b) 6.5 mm thickness

Fig. 5 Series of the RAA under different thickness.

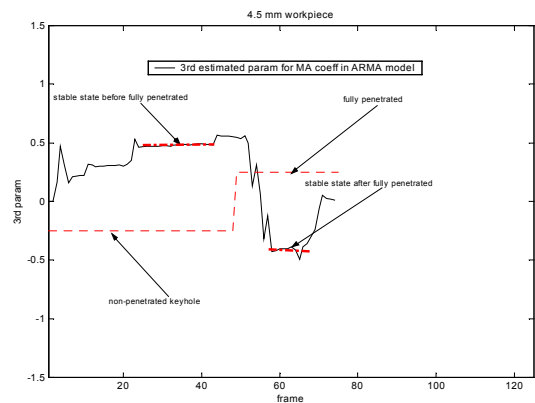
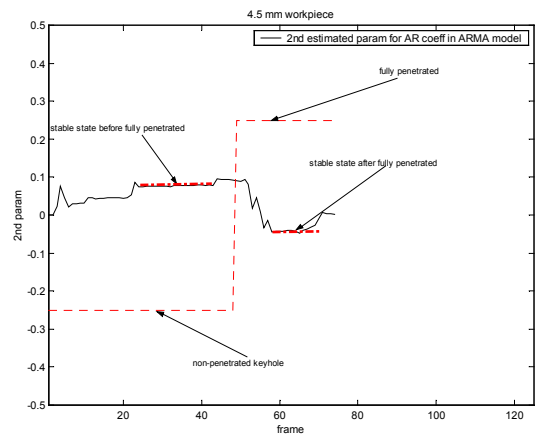
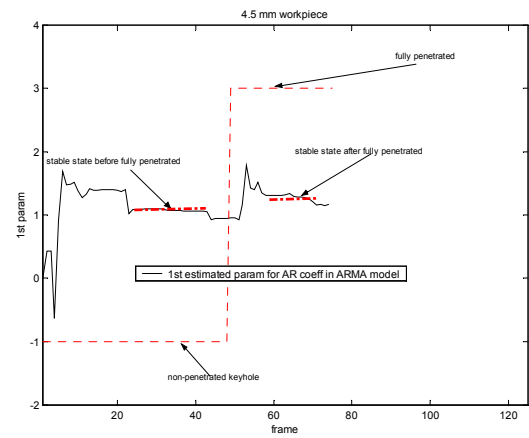


Fig. 6 Estimated parameters of data series under 4.5 mm thickness.

RAA exhibits different dynamic behaviors in different states. In the stable non-penetrated keyhole state, the non-penetrated keyhole grows and develops gradually; the geometry of the keyhole determines the RAA fluctuation. As a result, the RAA fluctuates, but with small amplitudes around a small angle. During the transition period, the geometry of the keyhole is subject to significant fluctuation. The RAA oscillates at large amplitudes. After the keyhole is settled into the stable penetrated keyhole state, the geometry of the keyhole maintains nearly unchanged. The RAA thus varies with very small amplitudes around a large reflection angle. Despite the characteristics of the RAA in different states, the RAA series in Fig. 5 looks too stochastic to determine the state. It appears no explicit function into

which the data set fits. Therefore, the data set should be considered a stochastic process and an auto-regressive moving-average (ARMA) model (Box and Jenkins,1994) is thus used to describe the RAA series $z(t)$:

$$\phi(B)z(t) = \theta(B)e(t) \quad (4)$$

where

$$\begin{cases} \phi(B) = 1 - \phi_1 B - \phi_2 B^2 - \dots - \phi_p B^p \\ \theta(B) = 1 - \theta_1 B - \theta_2 B^2 - \dots - \theta_q B^q \end{cases} \quad (5)$$

It was found that the RAA series can be described with a sufficient accuracy using an ARMA(2,1) model

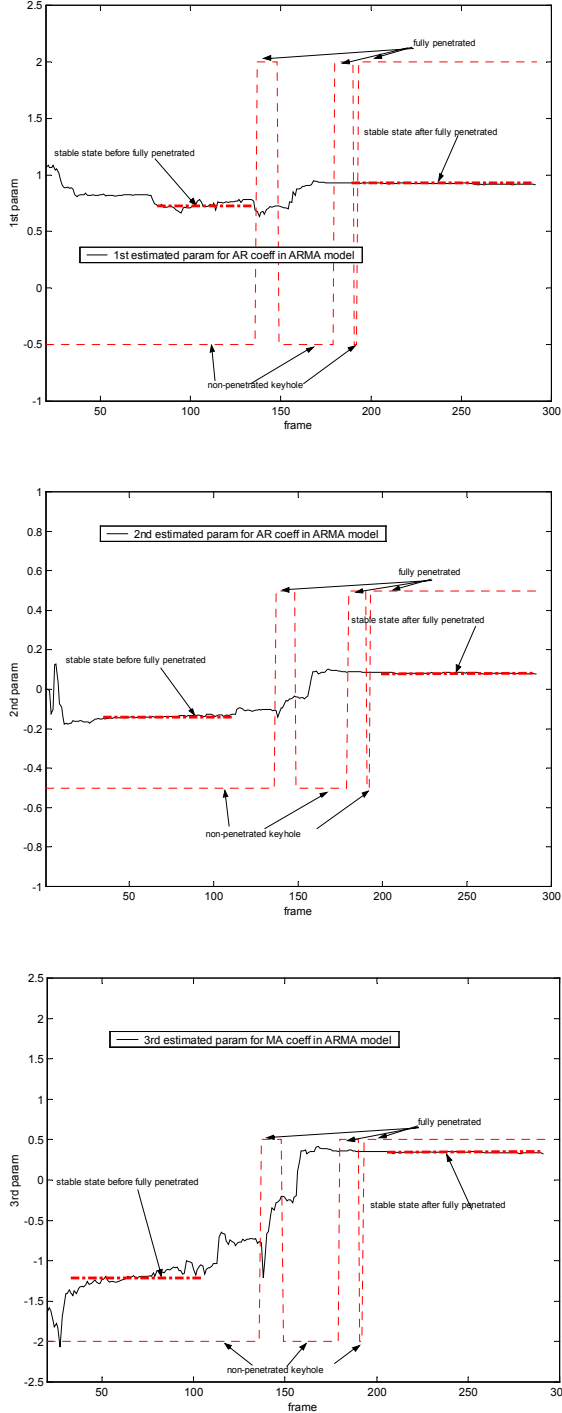


Fig. 7 Estimated parameters of data series under 6.5 mm thickness.

(Ma.,2001).

3. RECURSIVE ESTIMATION OF ARMA MODEL PARAMETERS

The ARMA(2,1) model can be written as

$$z(t) = \phi_1 z(t-1) + \phi_2 z(t-2) + \theta_1 e(t-1) + e(t) \quad (6)$$

Eq. (6) can be considered as a stochastic version of regression model. The parameter ϕ_1, ϕ_2, θ_1 can be recursively estimated by using the extended recursive least square algorithm (Astrom and Wittenmark,1995).

The regression model is:

$$z(t) = \begin{bmatrix} z(t-1) & z(t-2) & e(t-1) \end{bmatrix} \begin{bmatrix} \phi_1 \\ \phi_2 \\ \theta_1 \end{bmatrix} + e(t) \quad (7)$$

where $e(t-1)$ can be approximated by the predicted error

$$e(t-1) \approx \hat{e}(t-1) = z(t-1) - \begin{bmatrix} z(t-2) & z(t-3) & e(t-2) \end{bmatrix} \begin{bmatrix} \hat{\phi}_1(t-1) \\ \hat{\phi}_2(t-1) \\ \hat{\theta}_1(t-1) \end{bmatrix} \quad (8)$$

where $\hat{\theta}(t-1) = [\hat{\phi}_1(t-1), \hat{\phi}_2(t-1), \hat{\theta}_1(t-1)]^T$ is the recursive estimate of the parameter vector at the previous instant. Hence, the recursive equations are:

$$\begin{cases} \hat{\theta}(t) = \hat{\theta}(t-1) + p(t)\varphi(t-1)\varepsilon(t) \\ p(t) = \frac{1}{\lambda} \left[p(t-1) - \frac{p(t-1)\varphi(t-1)\varphi^T(t-1)p(t-1)}{\lambda + \varphi^T(t-1)p(t-1)\varphi(t-1)} \right] \end{cases} \quad (9)$$

where

$$\varepsilon(t) = z(t) - \hat{z}(t)$$

$$\hat{z}(t) = \varphi^T(t-1)\hat{\theta}(t-1) \quad (10)$$

$$\varphi(t-1) = \begin{bmatrix} z(t-1) & z(t-2) & e(t-1) \end{bmatrix}^T$$

$$\hat{\theta}(t-1) = \begin{bmatrix} \hat{\phi}_1(t-1) & \hat{\phi}_2(t-1) & \hat{\theta}_1(t-1) \end{bmatrix}^T$$

and λ is the forgetting factor.

4. ANALYSIS USING RECURSIVE ESTIMATES OF PARAMETERS

Fig. 6 shows the curves of the estimated parameters under thickness of 4.5 mm. It can be seen that at the beginning of the recursive estimation period, i.e., prior to frame 21, the estimates fluctuate. This is typical for recursive algorithms because of the large covariance gain. After this beginning period, the estimates become smooth. This indicates that the process is in a stable state. However, at approximately frame 50, the recursive estimates begin to change. This indicates a change in the development state of the keyhole. At approximately frame 60, the recursive estimates approach another stable state. Observation of the images (Ma.,2001) shows that the keyhole is first fully penetrated at frame 49. Also, the behavior of the reflected plasma reaches the stable penetrated keyhole state approximately at frame 61. As can be seen from the recursive estimates, the recursive estimates starts to change after frame 50 and become converged again at approximately frame 56. Hence, it is possible to use the

changes in the recursive estimates of the ARMA models to determine the change in the state of the development of the keyhole.

Fig. 7 shows the recursive estimates of the RAA during welding 6.5 mm thick work-piece. Observation of the images (Ma.,2001) shows that the keyhole is first fully penetrated at frame 113 and is finally settled at the new stable penetrated keyhole state at frame 169. Fig. 7 shows that the recursive parameters converged before frame 113. However, only θ_1 starts to change substantially right after frame 113. Other two parameters (ϕ_1, ϕ_2) start to substantially change after another 20 frames. In this case, although (ϕ_1, ϕ_2) did not change right after the first full penetration of the keyhole, the change in θ_1 was drastic. Such pattern in parameters can still suggest a very different ARMA process after frame 113. Hence, the transition period can still be predicted based on the recursive parameters. Further, approximately after frame 170, all the parameters converged again. This indicates that the process enters into another stable state. Of course, this state is of the stable penetrated keyhole.

It appears that the recursive estimates of the ARMA(2, 1) model can be used to determine the change in the state of the keyhole process. However, there are three parameters in an ARMA(2, 1) model. To determine the change in the state, three parameters need to be used as the inputs of a decision or discriminator function.

To propose a simple yet effective discriminator or decision function which determines the state of the keyhole process, let's consider the keyhole process as a system with a white noise as the input and the RAA as the output. The identified ARMA(2, 1) model is thus the impulse transfer function of the system. Denote the impulse transfer function as $H(z)$. Then,

$$H(z) = \frac{1 + \theta_1 z^{-1}}{1 - \phi_1 z^{-1} - \phi_2 z^{-2}} \quad (11)$$

The frequency response of the system is (Ziemer, et. al,1998):

$$H(e^{j\omega T}) = \frac{1 + \theta_1 e^{-j\omega T}}{1 - \phi_1 e^{-j\omega T} - \phi_2 e^{-j2\omega T}} \quad (12)$$

where ω is the frequency and T is the sampling period which is 0.001 second, i.e., one frame of image per millisecond, in this study. Hence, the recursive estimates of the parameters can be used to compute the system's frequency response at frequencies of interest.

The RAA series shown in Fig. 5 suggest that during the stable non-penetrated keyhole state, the RAA fluctuates with smaller amplitudes than it does during the transition period. The system which produces the RAA from the white noise should thus have higher high-frequency gains during stable non-penetrated keyhole than it has during the transition period. Further, in the stable penetrated-keyhole state, the fluctuation of the RAA is nearly negligible. The high-frequency gains must be the lowest while the low frequency gains must be the highest among the three states.

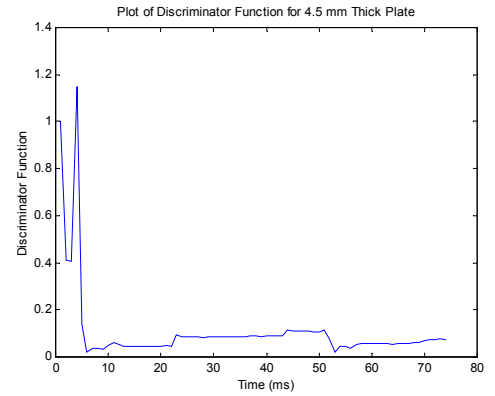
Based on the above discussion, a discriminator function is proposed below:

$$f = \left| \frac{H(e^{j\omega_H T})}{H(e^{j\omega_L T})} \right| \quad (13)$$

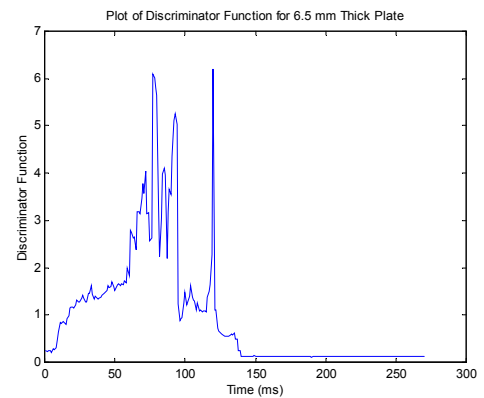
where ω_H and ω_L are the selected high and low frequency, respectively. Using $\omega_H = 2\pi \times 100$ rad/s and $\omega_L = 2\pi \times 10$ rad/s, the recursive estimates in Figs. 6 and 7 are used to compute the frequency responses at both the low and high frequency of selection and the discriminator function. The results are illustrated in Fig. 8(a) and Fig. 8(b) for the cases of 4.5 mm thick work-piece and 6.5 mm thick work-piece, respectively.

As can be seen in Fig. 8(a) for the thinner (4.5 mm thick) plate, the change in the state of the keyhole development can be determined from the discriminator function. In fact, the discriminator function decreases rapidly after frame 50 and settles after frame 56. This indicates that at frame 50, the keyhole process changes its state from the non-penetrated keyhole to the transition period. However, in this case (thinner plate), the duration of the transition period is very brief, and the process quickly enters into the stable penetrated keyhole state. Because of such a quick transition, one can consider that the process enters into the stable penetrated keyhole state directly from the stable non-penetrated keyhole state. The anticipated "middle" values of the discriminator function associated with the transition state is thus not observed.

Similarly, the change in the state of the keyhole development can be determined from the discriminator



(a) 4.5 mm thickness



(b) 6.5 mm thickness

Fig. 8 Discriminator function curves determined using recursive estimates of ARMA(2, 1) parameters.

function for the 6.5 mm thicker plate as can be seen in Fig. 8(b). Observation of the images (Ma.,2001) shows that the keyhole is fully penetrated at frame 113 and finally settles at the new stable penetrated keyhole state at frame 169. However, prior to frame 113, the reflection arc has started to increase its fluctuation amplitude. Such an increase in the fluctuation amplitude implies that the keyhole is about to fully penetrate. The keyhole process is thus about to change its state into the transition state. As can be seen in Fig. 8(b), the discriminator function sharply decreases prior to frame 98. This sudden decrease suggests that the keyhole has started its change from the stable non-penetrated keyhole to the transition period at frame 98. Hence, the discriminator function may provide a possible prediction, which is needed for advanced real-time control of the keyhole process, for the occurrence of the transition period in advance. On the other hand, observation of the images (Ma.,2001) shows that the keyhole opens and closes a few times before it finally settles at the stable penetrated keyhole state at frame 169. This type of fluctuation suggests a mixture of the transition state and the non-penetrated keyhole. Hence, the discriminator function may exhibit high values again during this period before the process finally settles at the stable penetrated keyhole state at frame 169. As can be seen, the discriminator function does exhibit high values again. However, such reoccurrence of high values only lasts a brief period and the discriminator function returns to the low values rapidly. Approximately at frame 140, the discriminator function decreases to a level which predicts the stable penetrated keyhole state.

As can be seen that for the thicker plate, the discriminator function is capable of predicting the change of the state in advance. This is primarily due to that the change of the state takes a long time to complete in the thicker plate. However, for the thinner plate, the change of the state completes much more quickly. Hence, for the thinner plate, the prediction function of the discriminator function is not pronounced although the change of the state can be determined based on the discriminator function. However, for specific applications, further studies must be conducted to learn specific dynamic behaviors of the reflection arc, which may vary with the travel speed of the welding torch, material, etc., in order to find the thresholds for automated prediction and determination of the change of the keyhole state.

5. CONCLUSIONS

This study used a high speed image processing system to acquire images during keyhole arc welding. The RAA was extracted from the image to describe the dynamic behaviors of the reflected plasma. It was found that the RAA series is a stochastic process which can be described using an ARMA model.

The parameters of the ARMA model were recursively estimated. It was found that the recursive estimates can converge if the state of the keyhole remains unchanged. However, if the state of the keyhole changes, at least some of the recursive estimates of the parameters substantially change accordingly. This implies that the parameters of the ARMA change upon the state of the keyhole.

The ARMA model can be considered the impulse transfer function of the ARMA system which produces RAA process from a white noise input. The frequency response of the ARMA system has different characteristics in different states. Based on the characteristics in the frequency response, a discriminator function can be formed to simplify the decision-making in detecting the state of the keyhole and improve the detection accuracy and robustness. For the thicker plate for which the change of the state takes certain time to complete, the discriminator function can also predict the change of the state in advance.

It should be pointed out that this study is focused on the development of the methodology. For specific applications, further studies must be done to determine the thresholds needed for automated prediction and determination of the change of the keyhole state.

ACKNOWLEDGEMENT

This work is funded by the United States' National Science Foundation under Grant DMI-9812981 and the Center for Robotics and Manufacturing Systems at the University of Kentucky.

REFERENCES

- Astrom, K. J. and B. Wittenmark (1995). *Adaptive Control*, 2nd Ed., Addison Wesley, Reading, MA.
- Box, G. E. P. and G. M. Jenkins (1994). *Time Series Analysis: Forecasting and Control*, Prentice Hall, Upper Saddle River, NJ.
- Ljung, L. (1997). *System Identification-Theory for the user*, 2nd Edition, Prentice Hall.
- Ma, Y. (2001). High Speed Image Based Stochastic Analysis of Dynamic Plasma Reflection Behavior. *MSEE. Thesis*, Department of Electrical and Computer Engineering, University of Kentucky, May.
- Zhang, Y. M., S. B. Zhang, and Y.C. Liu (2001). "Plasma cloud charge sensor for pulse keyhole process control", *Measurement Science and Technology*, **12(8)**: 1365-1370, 2001
- Ziemer, R. E., W. H. Tranter, and D. R. Fannin (1998). *Signals & Systems: Continuous and Discrete*, 4th Ed., Prentice Hall.